

RESEARCH ARTICLE

Crucial role of TRPC6 in maintaining the stability of HIF-1 α in glioma cells under hypoxia

Shanshan Li¹, Jinkui Wang², Yi Wei², Yongjian Liu², Xia Ding¹, Bin Dong^{2,*}, Yinghui Xu^{2,*} and Yizheng Wang^{1,*}**ABSTRACT**

Hypoxia-inducible factor-1 (HIF-1) is a key transcription factor responsible for the expression of a broad range of genes that facilitate acclimatization to hypoxia. Its stability is predominantly controlled by rapid hydroxylation of two proline residues in its α -subunit. However, how the rapid hydroxylation of HIF-1 α is regulated is not fully understood. Here, we report that transient receptor potential canonical (TRPC) 6 channels control hydroxylation and stability of HIF-1 α in human glioma cells under hypoxia. TRPC6 was rapidly activated by IGF-1R–PLC γ –IP₃R pathway upon hypoxia. Inhibition of TRPC6 enhanced the levels of α -ketoglutarate and promoted hydroxylation of HIF-1 α to suppress HIF-1 α accumulation without affecting its transcription or translation. Dimethylxalylglycine N-(methoxyoxoacetyl)-glycine methyl ester (DMOG), an analog of α -ketoglutarate, reversed the inhibition of HIF-1 α accumulation. Moreover, TRPC6 regulated GLUT1 (also known as SLC2A1) expression in a manner that was dependent on HIF-1 α accumulation to affect glucose uptake during hypoxia. Our results suggest that TRPC6 regulates metabolism to affect HIF-1 α stability and consequent glucose metabolism in human glioma cells under hypoxia.

KEY WORDS: α -Ketoglutarate, GLUT1, HIF-1 α , Hypoxia, TRPC6**INTRODUCTION**

All organisms must rapidly respond to hypoxia to survive. By regulating the ‘hypoxia signaling cascade’, hypoxia affects several processes, including energy metabolism, erythropoiesis, angiogenesis, cell proliferation and cell death (Oda et al., 2009). The transcription factor HIF-1 plays a central role in regulating expression of the genes involved in the processes. Induction of HIF-1 and subsequent activation of its target genes are the main cellular responses to hypoxia, which mediates numerous adaptive responses to both low physiological O₂ levels and various pathological conditions. HIF-1 regulates the expression of hundreds of genes in a cell-type-specific manner, and its complete transcriptome is likely to consist of thousands of genes (Semenza, 2007). It consists of the tightly regulated subunit HIF-1 α and constitutively expressed subunit HIF-1 β . HIF-1 α dimerizes with HIF-1 β and binds to hypoxia-response elements (HREs) in the promoters of target genes to modulate transcription of those genes. By regulating the expression of these genes, HIF-1 plays an important role in both physiological and pathological processes, such as embryogenesis,

tissue repair and tumorigenesis. Glucose transporter 1 (GLUT1, also known as SLC2A1), one of the HIF-1 target genes, is essential for glucose uptake in most cells, including tumor cells (Wertheimer et al., 1991; Ogura et al., 1999; Quintanilla et al., 2000; Porras et al., 2008; Chan et al., 2011). The increase in glucose uptake provides adequate energy and building blocks to promote tumor growth (Sebastián et al., 2012). Therefore, elucidating the mechanisms of HIF-1 α regulation is fundamentally important for understanding a variety of physiological and pathological processes, including tumor cell metabolism.

In normoxia, HIF-1 α is continuously and rapidly degraded. In the presence of O₂, Fe²⁺ and α -ketoglutarate, two conserved proline residues (Pro402 and Pro564) in the oxygen-dependent degradation domain (ODDD) of HIF-1 α are rapidly hydroxylated by HIF prolyl-hydroxylases (PHDs) and are recognized by the E3 ubiquitin ligase von Hippel Lindau protein (VHL), leading to the degradation of HIF-1 α by the ubiquitin–proteasome system (Andersson et al., 2010). Hypoxia inhibits PHDs, thereby suppressing HIF-1 α hydroxylation and degradation, and leading to its rapid accumulation (Benizri et al., 2008). However, how the rapid hydroxylation of HIF-1 α , the primary mechanism for controlling its stability and levels, is regulated is not fully understood.

In response to hypoxia, one of the initial changes in the cells is the rapid increase in intracellular Ca²⁺ concentration ([Ca²⁺]_i), which is due to both intracellular Ca²⁺ release and extracellular Ca²⁺ entry (Toescu, 2004). Reports have shown that increase of [Ca²⁺]_i during hypoxia enhances HIF-1 transcriptional activity (Mottet et al., 2003) and stimulates translation of HIF-1 α mRNA (Hui et al., 2006). However, whether the Ca²⁺ influx upon hypoxia affects the rapid hydroxylation of HIF-1 α still remains to be determined.

The TRPC6 channels, which are nonselective cation channels permeant to Ca²⁺, mediate Ca²⁺ elevation in tumor cells and have an important role in tumor development (Cai et al., 2009; Shi et al., 2009; Chigurupati et al., 2010; Ding et al., 2010; Monteith et al., 2012). In this study, we examined whether TRPC6 channels regulate HIF-1 α hydroxylation and stability in human glioma cells under hypoxia. We found that TRPC6 channels control metabolite levels to regulate the rapid hydroxylation of HIF-1 α and, hence, its stability, and in turn affect glioma cell glucose metabolism during hypoxia. Therefore, TRPC6 channels play a crucial role in maintaining HIF-1 α stability through metabolic regulation and affect the consequent metabolism in human glioma cells under hypoxia.

RESULTS**TRPC6 channels are required for hypoxia-induced HIF-1 α accumulation**

We initially investigated whether hypoxia-induced HIF-1 α expression is dependent on Ca²⁺ influx using human glioma cells as a model. HIF-1 α induction was rapid and peaked 4 h after hypoxia (1% O₂) and thereafter was maintained at an enhanced level

¹Laboratory of Neural Signal Transduction, Institute of Neuroscience, Shanghai Institutes of Biological Sciences, State Key Laboratory of Neuroscience, Chinese Academy of Sciences, Shanghai 200031, China. ²Department of Neurosurgery, 1st Affiliated Hospital of Dalian Medical University, Dalian 116011, China.

*Authors for correspondence (yzwang@ion.ac.cn, xuyh_dl@126.com, stocktondb@163.com)

(supplementary material Fig. S1A). Chelating the extracellular Ca^{2+} with ethylene glycol tetraacetic acid (EGTA) led to a concentration-dependent reduction in the hypoxic accumulation of HIF-1 α (supplementary material Fig. S1B). These results provided initial evidence to suggest that Ca^{2+} influx is important for the induction of HIF-1 α during hypoxia. To identify the channels responsible for the Ca^{2+} influx, we first adopted pharmacological approaches. Treatment of the cells with mibefradil (a T-type voltage-gated Ca^{2+} channel blocker), nimodipine (an L-type voltage-gated Ca^{2+} channel blocker), D-APV (an NMDA receptor antagonist) and CNQX (an AMPA and kainate glutamate receptor antagonist) did not change the enhancement in HIF-1 α levels induced by hypoxia. In contrast, treatment with SKF96365, a TRPC channel inhibitor, markedly suppressed the HIF-1 α induction (Fig. 1A). Collectively, these results suggest that Ca^{2+} influx mediated by TRPC channels likely plays a crucial role in HIF-1 α regulation.

As expression of TRPC6 among the TRPC family is specifically upregulated in human glioma tissues and is associated with glioma malignancy grades (Ding et al., 2010), we conducted different assays to examine the effect of TRPC6 on HIF-1 α levels. Downregulation of TRPC6 using two lentivirus-based short hairpin RNA (shRNA) sequences against human TRPC6 dramatically decreased hypoxia-induced HIF-1 α protein expression (Fig. 1B). To further test whether TRPC6 channel activity was indeed crucial for HIF-1 α expression, we examined the effect of a dominant-negative form of TRPC6 (DNC6), in which three mutations are introduced in its pore region to block the ion entrance (Hofmann et al., 2002), on hypoxia-induced HIF-1 α expression in different human glioma cell lines, including U251 (Fig. 1C) and U87 (supplementary material Fig. S1C) cells. Hypoxia markedly induced HIF-1 α protein accumulation in cells infected with GFP or wild-type TRPC6 (WTC6), whereas in DNC6-infected cells the induction was greatly suppressed (Fig. 1C; supplementary material Fig. S1C). However, DNC6 did not affect the accumulation of HIF-2 α protein during hypoxia (supplementary material Fig. S1D). Furthermore, treatment of the cells with CoCl_2 , a compound that is known to act as a chemical mimic to hypoxia, upregulated HIF-1 α expression and DNC6 suppressed CoCl_2 -induced HIF-1 α accumulation (Fig. 1D). Consistent with this, incubating the cells in a Ca^{2+} -free extracellular solution for 1 h abolished CoCl_2 -induced HIF-1 α accumulation (supplementary material Fig. S1E). It has been shown that chronic hypoxia (e.g. 4% O_2 for 40 h) upregulates TRPC6 expression in a manner that is partially mediated by HIF-1 (Lin et al., 2004; Wang et al., 2006; Liao et al., 2012). We examined TRPC6 expression in the glioma cells under normoxia or hypoxia (1% O_2) for 1–24 h. However, hypoxia did not increase TRPC6 expression. Instead, TRPC6 expression was decreased 8 h after hypoxia (supplementary material Fig. S1F). Taken together, these results suggest that Ca^{2+} influx through TRPC6 channels is crucial for hypoxia-induced HIF-1 α protein accumulation.

It has been reported that 1-oleoyl-2-acetyl-sn-glycerol (OAG), the membrane-permeant diacylglycerol (DAG) analog, can induce Ca^{2+} entry through TRPC6 (Chigurupati et al., 2010). We found that treatment of the cells with OAG increased HIF-1 α protein levels during normoxia, which was reversed by DNC6 (Fig. 1E). Taken together, these results suggest that TRPC6 is required for hypoxia-induced HIF-1 α expression in human glioma cells.

Activation of TRPC6 channels during hypoxia

We then studied whether TRPC6 is activated upon hypoxia in glioma cells. The Ca^{2+} imaging analysis showed that hypoxia induced an obvious intracellular Ca^{2+} elevation in U87 cells and that

the Ca^{2+} elevation in most of the cells oscillated (Fig. 2A; supplementary material Fig. S2A). When the cells were incubated in a Ca^{2+} -free extracellular solution, hypoxia only induced a slight intracellular Ca^{2+} elevation without the appearance of oscillation patterns (Fig. 2A), indicating that Ca^{2+} influx is important for the Ca^{2+} oscillations during hypoxia. Inhibition of TRPC6 by expression of shRNA (Fig. 2B) or DNC6 (Fig. 2C) suppressed the Ca^{2+} elevation, but did not apparently change the oscillation patterns. These results suggest that TRPC6 channels are responsible for intracellular Ca^{2+} elevation during hypoxia.

It is known that TRPC6 can be activated by either G-protein-coupled receptors (GPCRs) or receptor tyrosine kinases (RTKs) through mechanisms dependent on phospholipase C (PLC) β or γ , respectively (Montell, 2005; Tai et al., 2008). The activation of membrane-bound PLC results in the cleavage of phosphatidylinositol 4,5-bisphosphate (PIP_2) into inositol 1,4,5-trisphosphate (IP_3), which indirectly activates TRPC6 through the Ca^{2+} release from internal stores, and diacylglycerol (DAG), which can directly activate TRPC6. In the presence of thapsigargin, an inhibitor of the endoplasmic Ca^{2+} -ATPase known to deplete internal Ca^{2+} stores (supplementary material Fig. S2B), or 2-aminoethyl diphenylborinate (2-APB), an IP_3 receptor (IP_3R) antagonist (Fig. 2D), the hypoxia-induced intracellular Ca^{2+} elevation was almost completely suppressed. Therefore, it is likely that Ca^{2+} release from the internal stores mediated by the IP_3R contributes to the Ca^{2+} elevation in response to hypoxia. Moreover, treatment of the cells with U73122, a PLC antagonist, inhibited the Ca^{2+} elevation to the same extent as 2-APB (Fig. 2D). These results suggest that PLC is responsible for the Ca^{2+} elevation mediated by TRPC6.

We next studied the possible ligands released during hypoxia (Ghezzi et al., 1991; Ambalavanan et al., 1999; Michiels et al., 2000; Mouta Carreira et al., 2001; Hwang et al., 2007) that could stimulate GPCRs or RTKs to activate TRPC6 and mediate the hypoxia-induced intracellular Ca^{2+} elevation. Treatment of cells with 3-nitrocoumarin, an agent known to inhibit PLC γ activity without affecting PLC β , but not its inactive analog 7-OH-3-nitrocoumarin, substantially suppressed the Ca^{2+} elevation (Fig. 2E), suggesting that RTKs are involved in the intracellular Ca^{2+} elevation in response to hypoxia. Indeed, suramin, a general G protein antagonist, did not affect the Ca^{2+} elevation (supplementary material Fig. S2C). To determine which classes of RTKs, among the 20 different RTKs identified to date (Lemmon and Schlessinger, 2010), are activated during hypoxia we again used pharmacological agents, including: K252a, a nonspecific tropomyosin-related kinase (Trk) receptor inhibitor; pazopanib, an inhibitor for vascular endothelial growth factor receptors, platelet-derived growth factor receptors and fibroblast growth factor receptors; canertinib dihydrochloride, an ErbB inhibitor; and BMS-754807, an inhibitor for insulin-like growth factor-1 receptor (IGF-1R) and insulin receptor. As shown in supplementary material Fig. S2D,E, K252a and BMS-754807 significantly inhibited the Ca^{2+} elevation, indicating that the Trk receptors, IGF-1R and insulin receptor play a role in the hypoxia-induced intracellular Ca^{2+} elevation. As brain-derived neurotrophic factor (BDNF), a ligand for TrkB, can activate TRPC6 (Li et al., 2005; Jia et al., 2007; Tai et al., 2008), we tested whether BDNF and IGF-1 can be released and activate TRPC6 during hypoxia. The levels of IGF-1, but not those of BDNF, in the supernatants of the cells during hypoxia were greatly enhanced (Fig. 2F). Furthermore, IGF-1 induced an obvious intracellular Ca^{2+} elevation with oscillation patterns and the Ca^{2+} elevation was almost completely inhibited by DNC6 (Fig. 2G). To clearly show that IGF-

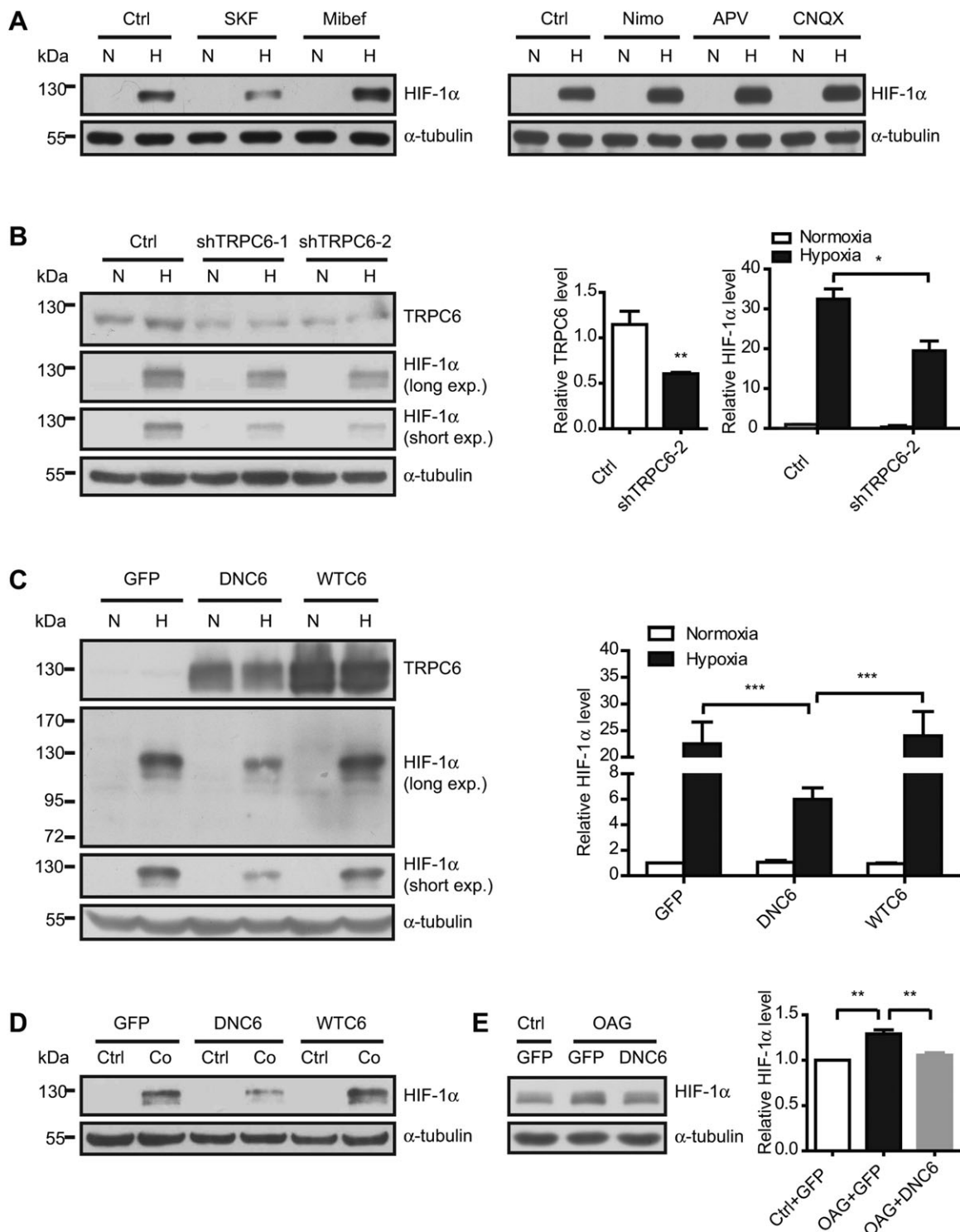


Fig. 1. TRPC6 is required for hypoxia-induced HIF-1 α accumulation. (A) Lysates of glioma cells cultured in normoxic (N) or hypoxic (H) conditions for 4 h in the presence of SKF96365 (SKF, 20 μ M), mibefradil (Mibef, 20 μ M), nimodipine (Nimo, 50 μ M), D-APV (APV, 100 μ M) or CNQX (25 μ M) were western blotted with the indicated antibodies. Ctrl, vehicle. (B) Representative western blot of the lysates from glioma cells transfected with control shRNA (Ctrl) or two TRPC6 shRNAs (shTRPC6-1, shTRPC6-2) and cultured in normoxic or hypoxic conditions for 4 h using the indicated antibodies. Right: quantification of TRPC6 and HIF-1 α protein levels. (C) Glioma cells infected with adenovirus expressing GFP, DNC6 or WTC6 and cultured in normoxic or hypoxic conditions for 4 h were extracted and subjected to western blot analysis using the indicated antibodies. Right: quantification of HIF-1 α protein levels. (D) Glioma cells were infected with adenovirus expressing GFP, DNC6 or WTC6 for 72 h and CoCl₂ (Co, 200 μ M) or vehicle (Ctrl) was added for 4 h. The cell extract was then prepared for western blotting using the indicated antibodies. (E) Glioma cells were infected with adenovirus expressing GFP or DNC6 for 72 h and OAG (100 μ M) or vehicle (Ctrl) was added for 4 h. The cell extract was then prepared for western blotting using the indicated antibodies. Right: quantification of HIF-1 α protein levels. Unless stated, glioma cells indicate U251 cells; normoxic (N) or hypoxic (H) condition is defined as 21% or 1% O₂, respectively. The data in B, C, E are shown as mean \pm s.e.m. from at least three independent experiments. For all experiments, α -tubulin was used as a loading control. * P <0.05, ** P <0.01, *** P <0.0001 [Student's t -test or ANOVA (more than two groups)].

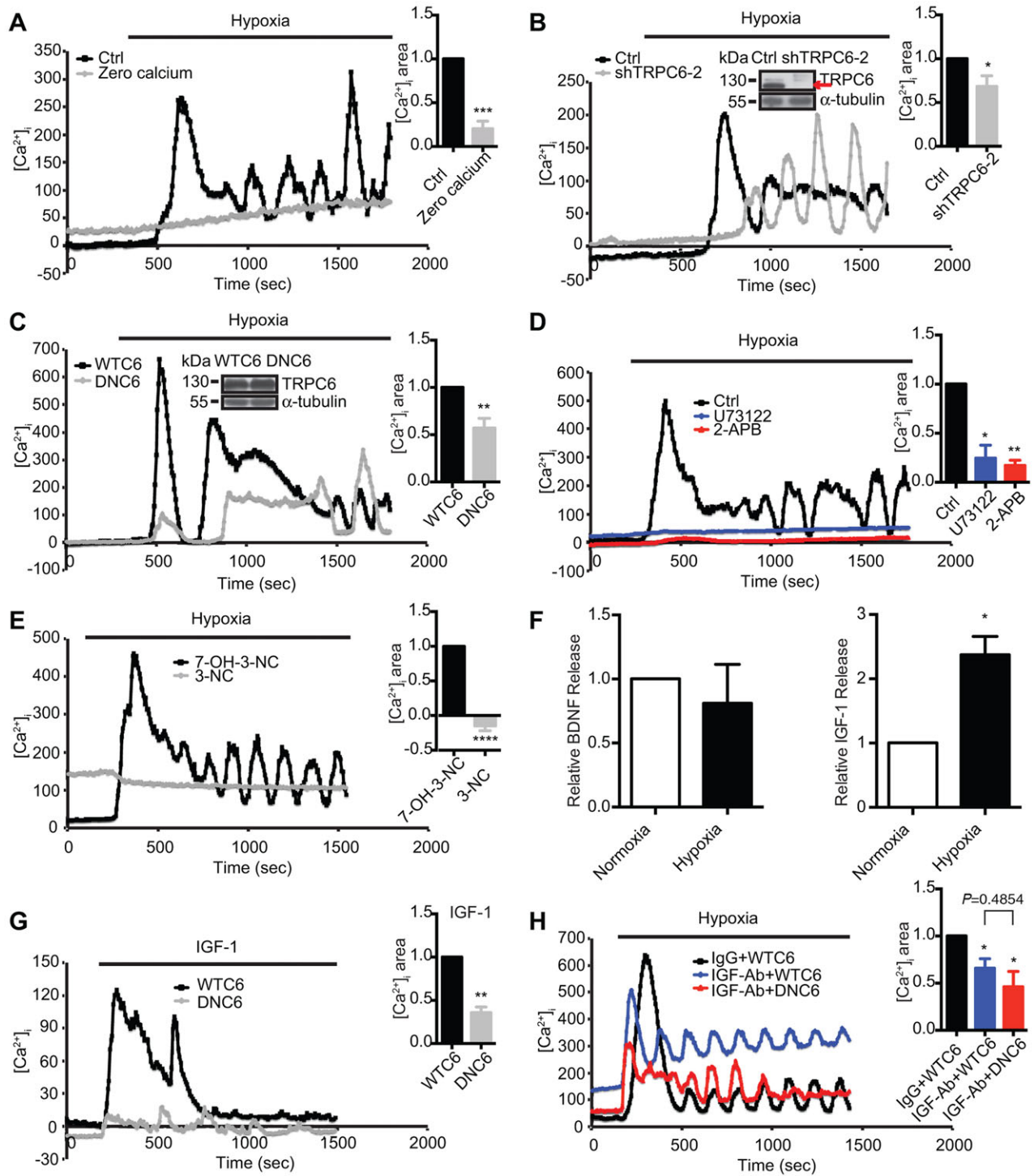


Fig. 2. TRPC6 contributes to intracellular Ca^{2+} elevation during hypoxia. (A) Representative traces of the intracellular Ca^{2+} elevation induced by hypoxia in U87 cells incubated without (Ctrl, $n=33$) or with (Zero calcium, $n=35$) a Ca^{2+} -free extracellular solution. $[\text{Ca}^{2+}]_i$ is in nM. The bar chart in this and subsequent panels shows a quantification of the Ca^{2+} elevation. (B) Intracellular Ca^{2+} elevation induced by hypoxia in U87 cells transfected with control shRNA (Ctrl, $n=31$) or TRPC6 shRNA (shTRPC6-2, $n=40$). (C) Intracellular Ca^{2+} elevation induced by hypoxia in U87 cells infected with adenovirus expressing WTC6 ($n=49$) or DNC6 ($n=49$). For B and C, representative blots for TRPC6 (red arrow in B) are shown in the inset. (D) Intracellular Ca^{2+} elevation induced by hypoxia in U87 cells treated with vehicle (Ctrl, $n=42$), U73122 (4 μM , $n=42$) or 2-APB (100 μM , $n=45$). (E) Intracellular Ca^{2+} levels induced by hypoxia in U87 cells treated with 7-OH-3-nitrocoumarin (7-OH-3-NC; 30 μM , $n=38$) or 3-nitrocoumarin (3-NC; 30 μM , $n=47$). (F) Supernatants of U87 cells cultured in normoxic or hypoxic conditions for 4 h were analyzed with ELISA kits. The levels of BDNF and IGF-1 in the hypoxic condition were normalized to those in normoxic condition. (G) Intracellular Ca^{2+} elevation induced by IGF-1 (1 $\mu\text{g}/\text{ml}$) in U87 cells infected with adenovirus expressing WTC6 ($n=60$) or DNC6 ($n=51$). (H) Intracellular Ca^{2+} elevation induced by hypoxia in U87 cells infected with adenovirus expressing WTC6 ($n=114$) or DNC6 ($n=64$) in the absence or presence of the monoclonal antibody 1H7 (sc-461) against the IGF-1R α -unit (IGF-Ab, 1:50). Drugs or antibodies were applied 20 min before exposure of cells to hypoxia unless otherwise indicated. The data are shown as mean \pm s.e.m. from at least three independent experiments. * $P < 0.05$, ** $P < 0.01$, *** $P < 0.001$, **** $P < 0.0001$ [Student's t -tests or ANOVA (more than two groups)].

1R mediates hypoxic effects on TRPC6 activation, we incubated cells with a neutralizing antibody (1H7) directed against the IGF-1R α -subunit to inhibit IGF-1R signaling (Kwon et al., 2009; Warnken et al., 2010) and examined the Ca^{2+} elevation. Neutralizing IGF-1 receptors did indeed suppress the hypoxia-induced intracellular Ca^{2+} elevation and DNC6 did not further inhibit the Ca^{2+} elevation (Fig. 2H).

Taken together, these results are consistent with an explanation that, during hypoxia, extracellular Ca^{2+} entry is triggered by the RTK-PLC γ -IP $_3$ R pathway, and TRPC6 channels are activated by this pathway to induce Ca^{2+} entry in human glioma cells.

Inhibition of TRPC6 increases HIF-1 α hydroxylation at Pro564 during hypoxia

It is known that HIF-1 α is hydroxylated at Pro402 and Pro564 by PHDs, leading to its proteasomal degradation during normoxia, whereas inhibition of the hydroxylations during hypoxia prevents the degradation, leading to its accumulation. We therefore studied whether TRPC6 channels affect HIF-1 α prolyl hydroxylation to promote its accumulation in glioma cells under hypoxia. When cells were treated with MG132, a potent proteasome inhibitor, the inhibition of HIF-1 α accumulation caused by DNC6 was reversed (supplementary material Fig. S3A), suggesting that TRPC6 regulation of HIF-1 α is dependent on the proteasome.

We then tested whether TRPC6 regulates HIF-1 α prolyl hydroxylation to affect its degradation using the anti-hydroxyl-HIF-1 α (Pro564) antibody. The specificity of the antibody to human hydroxyl-HIF-1 α was first verified. Treatment of HEK293 cells with MG132 induced hydroxylated HIF-1 α accumulation, whereas treatment with DMOG, an analog of α -ketoglutarate known to inhibit prolyl-4-hydroxylase activity, inhibited hydroxylation of HIF-1 α and enhanced its accumulation (supplementary material Fig. S3B). These results confirmed that this hydroxylation antibody could be used to examine hydroxyl-HIF-1 α .

When the cells were cultured in hypoxic conditions, the appearance of hydroxyl-HIF-1 α was evident (Fig. 3A, left). To clearly show that the effect of TRPC6 on HIF-1 α accumulation was due to an effect on its hydroxylation, we determined the ratio of hydroxyl-HIF-1 α (Pro564) to HIF-1 α (Hyp564:HIF-1 α), an approach used to evaluate the hydroxylation levels of HIF-1 α (Kageyama et al., 2004). Statistical analysis revealed that hypoxia decreased HIF-1 α hydroxylation and induced total HIF-1 α accumulation, whereas DNC6 increased HIF-1 α hydroxylation and suppressed total HIF-1 α accumulation during hypoxia (Fig. 3A, right). Moreover, 1 h after the induction of hypoxia, increased HIF-1 α hydroxylation was also found, which was sensitive to DNC6 (supplementary material Fig. S3C). Furthermore, the decrease in HIF-1 α hydroxylation seen upon treatment of the cells with OAG during normoxia could be reversed by DNC6 (Fig. 1E; supplementary material Fig. S3D). These findings suggest that inhibition of TRPC6 promotes the rapid prolyl hydroxylation of HIF-1 α during hypoxia. To test this hypothesis, cells were transfected with genetically modified HIF-1 α in which the two proline residues were mutated to alanine and glycine residues, respectively (P402A/P564G), to prevent their hydroxylation (Kageyama et al., 2004). We found that DNC6 suppressed wild-type HIF-1 α protein during hypoxia, whereas it did not affect the protein levels of HIF-1 α when the two mutations were introduced (Fig. 3B). These results thus support an explanation that TRPC6 inhibits HIF-1 α prolyl hydroxylation to promote its stability during hypoxia.

We also determined whether TRPC6 affects HIF-1 α mRNA translation and accumulation. The hypoxia-induced HIF-1 α mRNA

translation is cap-dependent, mediated mainly through the PI3K–Akt–mTOR and Ras–MEK–ERK1/2 pathways (Hui et al., 2006; Galban and Gorospe, 2009). Once activated, two substrates, p70 S6 kinase and the translation initiation factor eIF4E-binding protein (4E-BP1), are phosphorylated to maintain active translation initiation. We found that when TRPC6 was inhibited, the activation of p70 S6K, 4E-BP1, ERK1/2 and Akt, as evidenced by their phosphorylation, was not changed or only slightly increased during hypoxia (Fig. 3C; supplementary material Fig. S3E), indicating that these pathways cannot be accountable for the DNC6-mediated inhibition of HIF-1 α accumulation during hypoxia. In addition, HIF-1 α mRNA levels were greatly reduced in GFP-, WTC6- or DNC6-infected cells during hypoxia (Fig. 3D). These findings suggest that HIF-1 α mRNA transcription and translation are unlikely to be responsible for the effect of TRPC6 on HIF-1 α accumulation during hypoxia.

Taken together, our results are consistent with an explanation that TRPC6 increases HIF-1 α accumulation by suppressing its hydroxylation rather than by affecting its transcription or translation in human glioma cells under hypoxia.

TRPC6 alters metabolite levels during hypoxia

We next explored how TRPC6 channels regulate HIF-1 α prolyl hydroxylation. In normoxia, HIF-1 α is hydroxylated by PHDs at Pro402 and Pro564 in a reaction requiring α -ketoglutarate, O_2 and Fe^{2+} (Berra et al., 2003). The PHD activities can be inhibited by succinate, fumarate and 2-hydroxyglutarate through competitive inhibition and/or product inhibition (Pollard and Ratcliffe, 2009; Zhao et al., 2009; Xu et al., 2011; Oermann et al., 2012). We thus used ^1H nuclear magnetic resonance (^1H NMR) to measure the intracellular levels of these metabolites in glioma cells under hypoxia. We found that when TRPC6 was inhibited, the α -ketoglutarate levels were markedly enhanced, whereas fumarate levels were greatly suppressed (Fig. 4A). Alterations in these metabolites are known to increase PHD activities (Oermann et al., 2012), as was verified by the finding that addition of cell-permeable dimethyl α -ketoglutarate promoted HIF-1 α hydroxylation during hypoxia (supplementary material Fig. S3F). However, the lactate levels were not changed. These findings provide initial evidence that TRPC6 can regulate metabolite levels to affect the stability of HIF-1 α . To directly show the possible role of α -ketoglutarate in mediating the effect of TRPC6 on HIF-1 α accumulation, we treated the cells with DMOG, an analog of α -ketoglutarate known to inhibit PHD activities, and examined HIF-1 α expression. As shown in Fig. 4B and supplementary material Fig. S3G, the inhibition of HIF-1 α accumulation observed in DNC6-infected cells under hypoxia was mostly reversed in the presence of DMOG. We also knocked down fumarase, which catalyzes the conversion of fumarate, another competitive inhibitor of PHDs, into malate, with lentiviral shRNA. Expression of the shRNA dramatically decreased the levels of overexpressed fumarase and blocked DNC6-mediated inhibition of HIF-1 α accumulation under hypoxia in a manner similar to the effect of DMOG on HIF-1 α accumulation (Fig. 4C). Taken together, these results show that inhibition of TRPC6 causes increase in α -ketoglutarate levels and reduction in fumarate levels, leading to PHD-mediated hydroxylation and degradation of HIF-1 α during hypoxia.

As α -ketoglutarate dehydrogenase (α -KGDH, also known as OGDH), an enzyme known to convert α -ketoglutarate into succinyl-CoA, can be directly activated by Ca^{2+} , and inhibition of its activity increases α -ketoglutarate levels (Nichols and Denton, 1995; Gunter et al., 2000; Satrustegui et al., 2007), we examined whether TRPC6

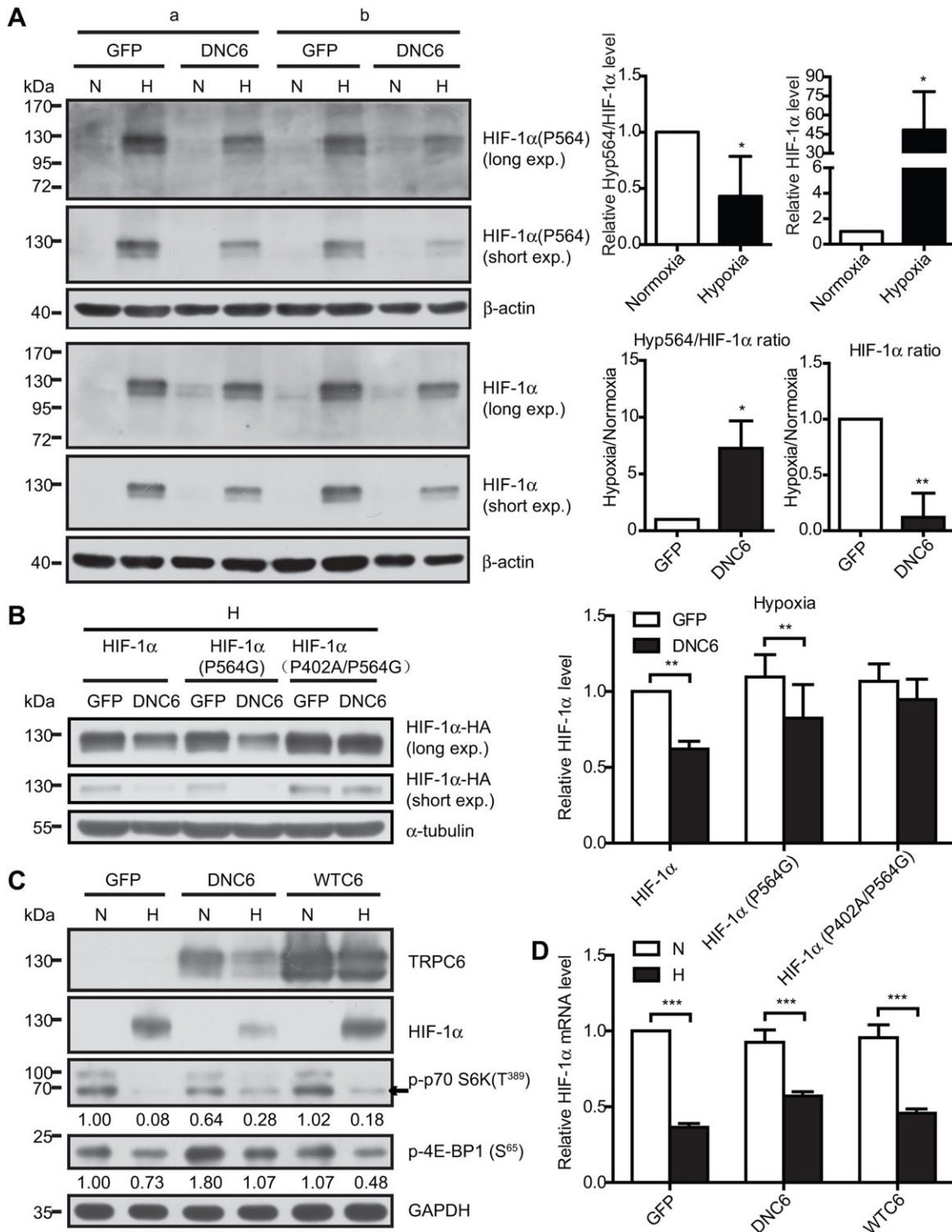


Fig. 3. Inhibition of TRPC6 promotes prolyl hydroxylation of HIF-1 α during hypoxia. (A) Lysates of glioma cells infected with adenovirus expressing GFP or DNC6 and cultured in normoxic (N) or hypoxic (H) conditions for 4 h were western blotted using the antibody against hydroxylated form of HIF-1 α at proline 564 (P564). 'a' and 'b' represent two independent experiments. Right: upper, quantification of hydroxylation levels of HIF-1 α and HIF-1 α levels in the cells infected with GFP; lower, quantification of hydroxylation levels of HIF-1 α during hypoxia [(Hyp564/HIF-1 α during hypoxia)/(Hyp564/HIF-1 α in normoxia)], and quantification of HIF-1 α levels during hypoxia [(HIF-1 α during hypoxia)/(HIF-1 α in normoxia)]. (B) Glioma cells transfected with pCAGGS-HIF-1 α -HA or its mutants as indicated along with adenovirus expressing GFP or DNC6 and cultured in hypoxic condition for 4 h were extracted and subjected to western blotting using anti-HA antibody. Right: quantification of HIF-1 α protein levels. (C) Effects of DNC6 on phosphorylation (p-) of p70 S6K or 4E-BP1 were analyzed by western blotting using the indicated antibodies and the relative amount of them determined by densitometry is shown below the blot. (D) Total RNA isolated from glioma cells infected with adenovirus expressing GFP, DNC6 or WTC6 in normoxic or hypoxic conditions for 4 h was assayed by qPCR analysis using primers for HIF-1 α . The levels of HIF-1 α mRNA were normalized to that of GAPDH. The data are shown as mean+s.e.m. from at least three independent experiments. * P <0.05, ** P <0.01, *** P <0.001 [Student's t -test or ANOVA (more than two groups)].

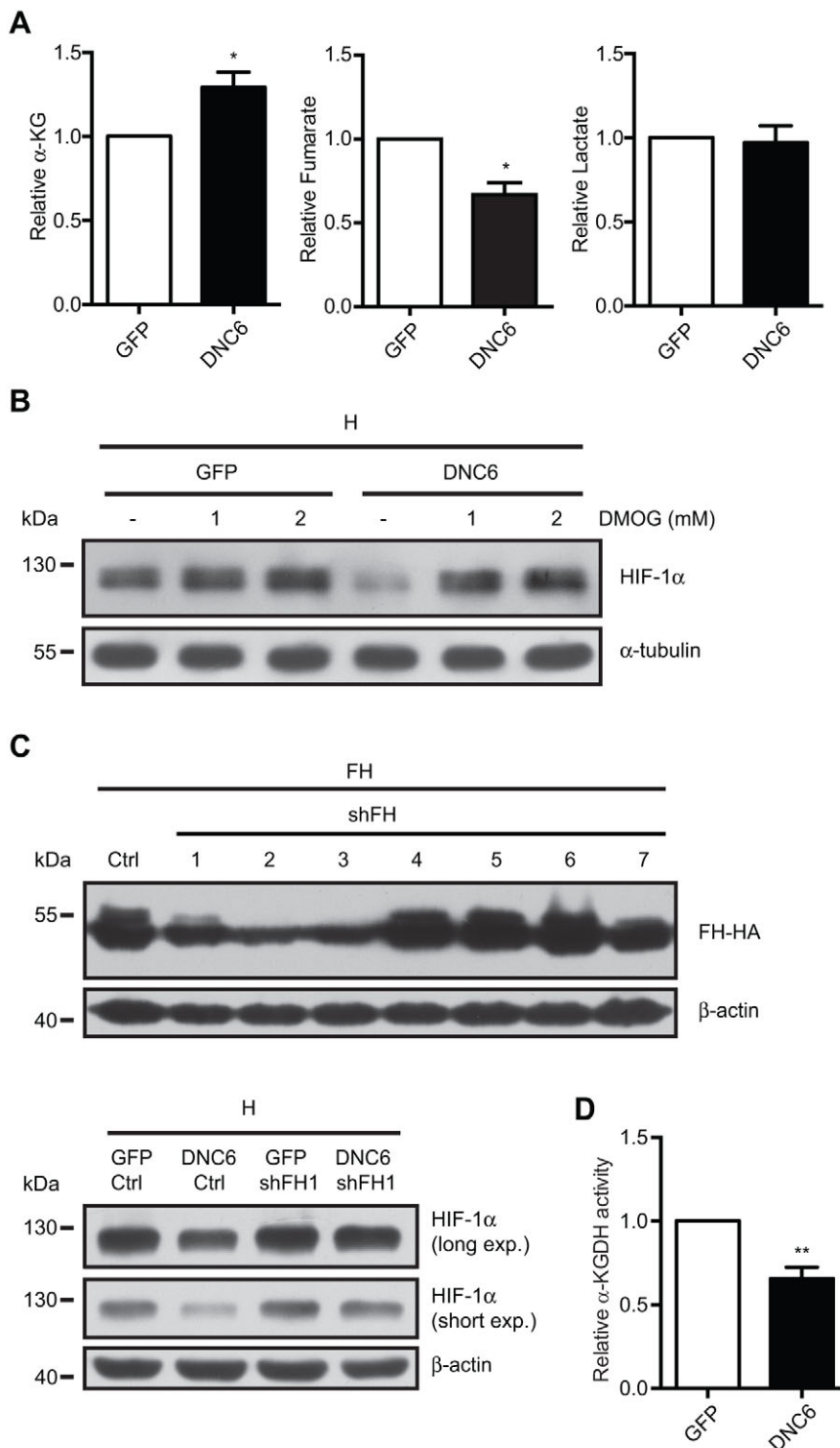


Fig. 4. TRPC6 regulates metabolite levels to control HIF-1 α protein levels. (A) Glioma cells infected with adenovirus expressing GFP or DNC6 and cultured in hypoxic condition were extracted for ^1H NMR analysis. The levels of the indicated metabolites in the cells infected with DNC6 were measured and normalized to those in the cells infected with GFP. α -KG, α -ketoglutarate. Data are shown as mean+s.e.m. from three independent experiments. (B) Glioma cells infected with adenovirus expressing GFP or DNC6 and cultured in hypoxic conditions for 4 h in the presence or absence of DMOG were extracted and subjected to western blot analysis using the indicated antibodies. (C) Upper: glioma cells transfected with pCAGGS-FH-HA (encoding HA-tagged fumarase, HA-FH) along with control shRNA (Ctrl) or fumarase shRNA (shFH1–shFH7) for 72 h were extracted and subjected to western blotting using the anti-HA antibody. Lower: glioma cells infected with adenovirus expressing GFP or DNC6 were transfected with control shRNA or fumarase shRNA (shFH1) and cultured in hypoxic condition for 4 h. The cell extract was then prepared for western blotting using the indicated antibodies. (D) Glioma cells infected with adenovirus expressing GFP or DNC6 and cultured in hypoxic conditions for 4 h were extracted for GC-MS analysis. The ratio of succinate to α -ketoglutarate was used to evaluate the activity of α -KGDH, and α -KGDH activity in the cells infected with DNC6 was normalized to that in the cells infected with GFP. Data are shown as mean+s.e.m. from four independent experiments. * P <0.05, ** P <0.01 (Student's t -test).

affects the activity of α -KGDH to regulate α -ketoglutarate levels. We used a gas chromatography mass spectrometer (GC-MS) to determine the intracellular levels of α -ketoglutarate and succinate because the ratio of succinate to α -ketoglutarate can be used to evaluate α -KGDH activity. Consistent with the results shown in Fig. 4A, when TRPC6 was inhibited, the ratio of succinate to α -ketoglutarate was markedly lowered during hypoxia (Fig. 4D). These results suggest that α -KGDH activity is suppressed by DNC6. Taken together, our results thus support the hypothesis that

TRPC6 controls the production of metabolites to regulate the stability of HIF-1 α in human glioma cells under hypoxia.

TRPC6 promotes glucose uptake during hypoxia in a manner that is dependent on HIF-1 α

The above results suggest that TRPC6 could regulate the metabolism of cells to control the stability of HIF-1 α during hypoxia. Because it is believed that cell metabolism plays an important role in different physiological or pathological processes (Zhang et al., 2013; Charitov

et al., 2015), we next studied whether TRPC6 regulates HIF-1 α stability to affect the metabolism of glioma cells during hypoxia. We searched The Cancer Genome Atlas (TCGA) database (Brennan et al., 2013), and analysis of the expression data in human glioblastoma samples revealed that the mRNA expression of solute carrier family 2, facilitated glucose transporter member 1 (*SLC2A1*), lactate dehydrogenase A (*LDHA*) and lactate dehydrogenase B (*LDHB*), three well-known genes involved in energy metabolism (Sharp and Bernaudin, 2004), was highly correlated with the mRNA expression of *TRPC6* (supplementary material Fig. S4A). These results suggest that TRPC6 might have a role in the control of glucose metabolism in human glioma. To further study this possibility, we examined the expression of these three genes in human glioma cell lines under both normoxia and hypoxia. As shown in supplementary material Fig. S4B, mRNA levels for *SLC2A1* and *LDHA*, but not *LDHB*, were greatly enhanced during hypoxia. However, expression of DNC6 only suppressed hypoxia-induced *SLC2A1* mRNA levels without affecting *LDHA* expression, suggesting that TRPC6 specifically controls *SLC2A1* expression in these cultured cells during hypoxia.

We then determined whether TRPC6 regulates metabolism to control the expression of *SLC2A1*, whose product, GLUT1, is responsible for glucose uptake. Results in Fig. 5A show that the inhibitory effect of DNC6 on *SLC2A1* mRNA levels during hypoxia was reversed in the presence of DMOG. Consistent with this, expressing DNC6 suppressed the hypoxia-induced increase in GLUT1 protein levels and DMOG reversed the inhibition (Fig. 5B; supplementary material Fig. S4C).

It is known that expression of *SLC2A1* during hypoxia is mediated by HIF-1 α (Sharp and Bernaudin, 2004; Chan et al., 2011; Ferrer et al., 2014). To clearly show that HIF-1 α mediates the effect of TRPC6 on GLUT1 expression, we transfected glioma cells with exogenous HIF-1 α to specifically upregulate its expression. Expressing HIF-1 α indeed reversed DNC6-mediated inhibition of GLUT1 expression during hypoxia (Fig. 5C). We then explored the biological role of TRPC6-induced HIF-1 α in regulation of glucose uptake (Fig. 5D). The glucose uptake in normoxia was greatly enhanced when HIF-1 α expression was increased. However, it was not changed when TRPC6 was inhibited in the cells. Hypoxia treatment led to a great increase in glucose uptake and expressing DNC6 suppressed the enhancement. Moreover, expressing HIF-1 α reversed the DNC6-mediated suppression of glucose uptake in a manner similar to its effects on GLUT1 expression. These results suggest that TRPC6 promotes glucose uptake through HIF-1 α during hypoxia.

Furthermore, treatment of the cells with OAG increased *SLC2A1* mRNA and GLUT1 protein levels during hypoxia (Fig. 5E), which was dramatically decreased by expressing DNC6 (supplementary material Fig. S4D). Collectively, these results suggest that activation of TRPC6 channels enhances glucose uptake in a manner that is mediated by HIF-1 α in human glioma cells under hypoxia.

DISCUSSION

In this study, we showed that hypoxia in glioma cells induces sequential responses, including release of IGF-1, activation of TRPC6 channels, changes in the metabolite levels and maintenance of HIF-1 α stability, leading to an increase in glucose metabolism (supplementary material Fig. S4E). Several lines of experimental results support this conclusion. First, IGF-1 was specifically released in human glioma cells during hypoxia. Second, TRPC6 channels were rapidly activated by the IGF-1R–PLC γ –IP $_3$ R pathway and inhibition of TRPC6 greatly suppressed the

intracellular Ca $^{2+}$ elevation during hypoxia. Third, inhibition of TRPC6 promoted HIF-1 α hydroxylation to suppress HIF-1 α accumulation during hypoxia, but did not affect its transcription or translation. Fourth, inhibition of TRPC6 increased α -ketoglutarate levels and promoted PHD activities, leading to HIF-1 α degradation during hypoxia. Finally, TRPC6 regulated GLUT1 mRNA and protein levels through HIF-1 α to affect glucose uptake during hypoxia. Therefore, TRPC6 controls the metabolite levels to regulate the rapid hydroxylation and stability of HIF-1 α , and affect the consequent glucose metabolism during hypoxia. In this context, TRPC6 can act as an important metabolic regulator.

As one of the rapid cellular responses to hypoxia, an intracellular Ca $^{2+}$ elevation in different types of cells has been reported (Hu and Ziegelstein, 2000; Jin et al., 2005) and most of the Ca $^{2+}$ elevations exhibit oscillation patterns. The mechanisms underlying Ca $^{2+}$ oscillations are quite different between different cell types. It is believed that the Ca $^{2+}$ elevation with an oscillation pattern results from both Ca $^{2+}$ influx and Ca $^{2+}$ release (Sneyd et al., 1995; Marhl et al., 2000; Dupont et al., 2011). Studies have shown that three types of Ca $^{2+}$ channels in the plasma membrane, including the TRP channels, contribute to the increase in [Ca $^{2+}$] $_i$ under hypoxia (Toescu, 2004; Meng et al., 2008). Here, in human glioma cells, we found that TRPC6 activated by the IGF-1R–PLC γ –IP $_3$ R pathway was responsible for hypoxia-induced Ca $^{2+}$ entry (Fig. 2). IGF-1 released during hypoxia stimulates IGF-1R, leading to the activation of PLC γ , which hydrolyzes PIP $_2$ into DAG and IP $_3$. IP $_3$ induces Ca $^{2+}$ release from internal stores, which in turn activates TRPC6 to mediate Ca $^{2+}$ influx. This sequential response is likely accountable for the delay in the time until the response starts after hypoxia. Although DAG is known to activate TRPC6 (Nilius and Voets, 2005; Pedersen et al., 2005; Nilius et al., 2007), in some studies TRPC6 activation is also linked to internal Ca $^{2+}$ release (Jia et al., 2007; Brécharde et al., 2008). Here, we showed again that Ca $^{2+}$ release from the internal stores, rather than DAG, activated TRPC6 during hypoxia (Fig. 2D; supplementary material Fig. S2B). Therefore, Ca $^{2+}$ influx through TRPC6 during hypoxia contributed to the Ca $^{2+}$ elevation and the subsequent rapid inhibition of HIF-1 α hydroxylation in the glioma cells (Fig. 2C, supplementary material Fig. S3C). It should be mentioned that when TRPC6 was inhibited, OAG-induced HIF-1 α expression was completely suppressed (Fig. 1E), whereas hypoxia-induced HIF-1 α expression was greatly, but not completely, suppressed (Fig. 1C), suggesting that TRPC6 activation is a key cellular response to hypoxia. It should be pointed out that inhibition of TRPC6 suppressed the hypoxia-induced Ca $^{2+}$ elevation, but did not affect the hypoxia-induced Ca $^{2+}$ oscillation patterns. In addition, because neutralizing IGF-1R partially blocked the hypoxia-induced Ca $^{2+}$ elevation and DNC6 abolished the IGF-1-induced Ca $^{2+}$ elevation (Fig. 2G,H), it is possible that other RTKs are also responsible for TRPC6 activation and Ca $^{2+}$ elevation during hypoxia.

An important finding of the current study is that TRPC6 regulates metabolite levels to further affect glucose metabolism. Although TRPC6 affects α -ketoglutarate production to regulate HIF-1 α hydroxylation, unexpectedly, we observed the appearance of hydroxyl-HIF-1 α upon hypoxia (Fig. 3A). Similar findings have also been reported previously (Chan et al., 2002). In normoxia, the E3 ubiquitin ligase VHL targets hydroxyl-HIF-1 α for proteasomal degradation. It has been reported that hypoxia upregulates PIASy (also known as PIAS4), a SUMO E3 ligase, to inactivate VHL (Cai et al., 2010) or decrease VHL protein levels (Liu et al., 2011). Therefore, it is possible that hypoxia inhibits the activity of VHL,

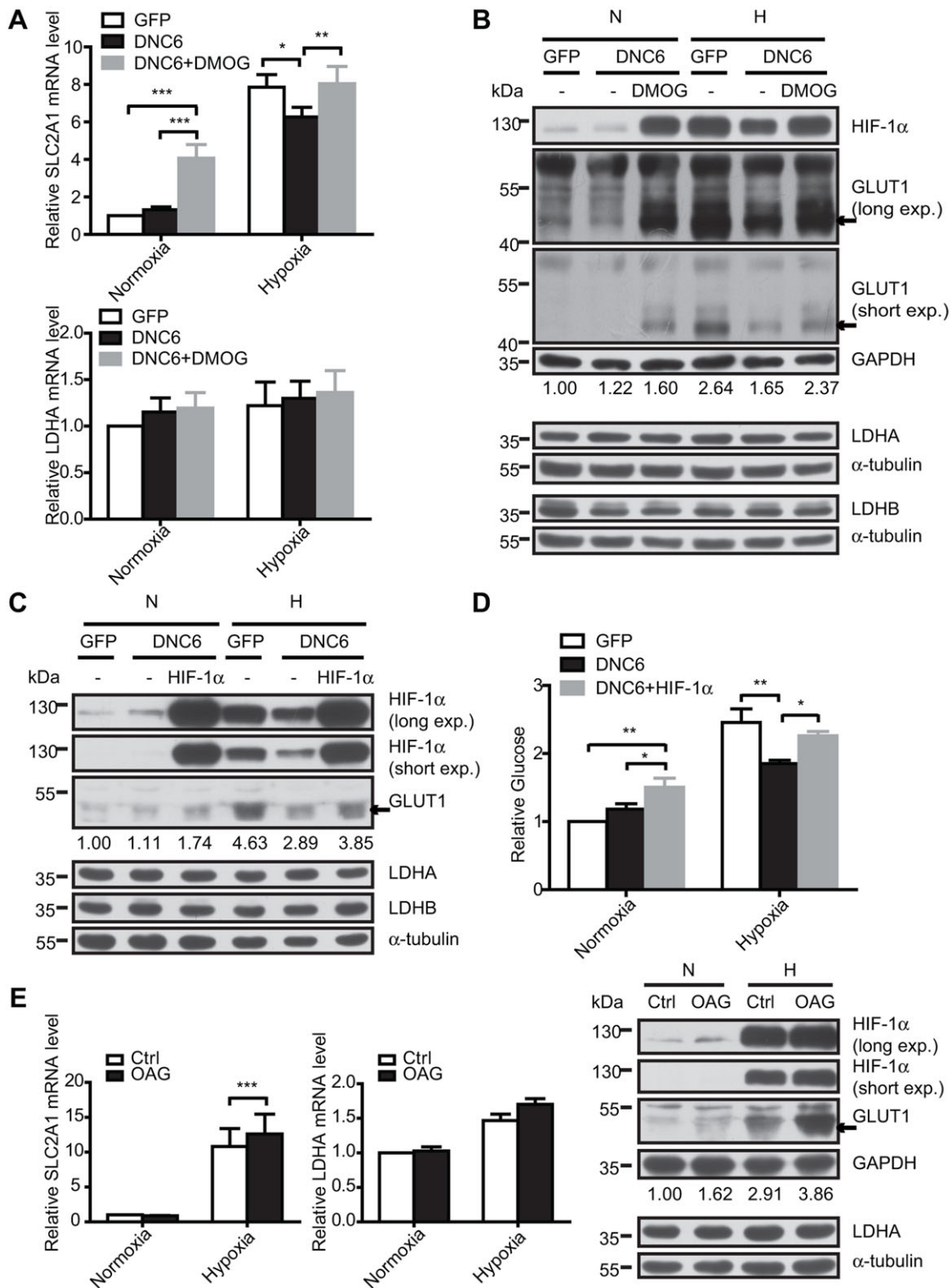


Fig. 5. TRPC6 promotes glucose uptake during hypoxia in a manner that is dependent on HIF-1 α . (A,B) U87 cells infected as indicated and cultured in normoxic (N) or hypoxic (H) conditions for 24 h in the presence or absence of DMOG (0.5 mM) were extracted for qPCR analysis using the primers for *SLC2A1* and *LDHA* (A) or for western blot analysis using the indicated antibodies (B). The corresponding mRNA levels were normalized to GAPDH levels. Data are shown as mean+s.e.m. from four (*SLC2A1*) or five (*LDHA*) independent experiments. The relative amount of GLUT1 determined by densitometry is shown below the blot. (C) U87 cells infected as indicated were transfected with or without pCAGGS-HIF-1 α -HA and cultured in normoxic or hypoxic conditions for 24 h. The cell extract was then prepared for western blotting using the indicated antibodies. (D) Intracellular glucose levels were measured from the cells as in C and normalized to those from the cells infected with GFP and subjected to normoxia. Data are shown as mean+s.e.m. from three independent experiments. (E) Left: total RNA isolated from U87 cells cultured in normoxic or hypoxic conditions for 8 h in the presence or absence of OAG (100 μ M) was assayed by qPCR analysis. Data are shown as mean+s.e.m. from four independent experiments. Right: cell lysates from U87 cells cultured in normoxic or hypoxic conditions for 24 h in the presence or absence of OAG (50 μ M) were western blotted with the indicated antibodies. The black arrows indicate GLUT1. * P <0.05, ** P <0.01, *** P <0.001 (ANOVA).

leading to the appearance of hydroxyl-HIF-1 α under hypoxia in these glioma cells.

One of the important implications of the current study is that other α -ketoglutarate-dependent regulations could be also affected by TRPC6 channel activity. It is known that, in addition to PHDs being involved in HIF-1 α degradation, many other dioxygenases utilize α -ketoglutarate as a co-substrate in mammalian cells to affect cellular activities, such as the histone demethylases with JmjC domain (JHDMs) and DNA hydroxylases in the form of ten-eleven translocases (TETs) that convert 5-methylcytosine into 5-hydroxymethylcytosine (Xu et al., 2011; Oermann et al., 2012). The JHDMs cause genome-wide increases or decreases in histone methylation (Krieg et al., 2010; Kaelin and McKnight, 2013). TETs generate 5-hydroxymethylcytosine, which serves as an intermediate of DNA demethylation (Kaelin and McKnight, 2013; Mariani et al., 2014). Both of them play crucial roles in epigenetic gene regulation. Therefore, as TRPC6 plays an important role in regulation of α -ketoglutarate-dependent PHD activities to modulate the stability of HIF-1 α , other α -ketoglutarate-dependent dioxygenases might be also regulated by Ca²⁺ influx through TRPC6 to result in a plethora of cellular responses.

Increased glucose uptake is an important metabolic characteristic of proliferating cells as well as tumor cells, and has been applied to tumor diagnosis (DeBerardinis and Thompson, 2012). Glucose is used to generate ATP as well as biomass. This means that, besides supplying free energy, some glucose is diverted to form macromolecular precursors, such as ribose for nucleotides (if diverted to the pentose phosphate pathway), glycolytic intermediates for amino acids and acetyl-CoA for fatty acids (Vander Heiden et al., 2009). HIF-1 α plays a crucial role in tumor cell glucose metabolism by regulating the expression of the metabolism-related genes (Faubert et al., 2013; Yang et al., 2014). The fact that TRPC6 regulated the HIF-1 α -mediated GLUT1 expression and glucose uptake under hypoxia without affecting lactate levels in glioma cell lines (Fig. 4A; Fig. 5) suggests that TRPC6 promotes glucose metabolism during hypoxia but, however, does not stimulate LDHA-mediated glycolysis to produce energy. It is therefore plausible that the glucose taken up through TRPC6 regulation is likely used for the biosynthesis of macromolecules in the cultured cells. It should be pointed out that some of these results in cultured cells were not consistent with the data from TCGA (supplementary material Fig. S4A), suggesting that cell metabolism *in vitro* and *in vivo* could be different. Numerous studies have reported that all major tumor suppressors and oncogenes have a profound effect on metabolic pathways, particularly glucose metabolism (Cairns et al., 2011; Koppenol et al., 2011). In this report, we provide evidence that Ca²⁺ signaling initiated by TRPC6 can also regulate tumor cell glucose metabolism. In addition, the inhibitory effect of DNC6 on GLUT1 expression might partially explain its suppression of tumor cell development (Cai et al., 2009; Shi et al., 2009; Chigurupati et al., 2010; Ding et al., 2010; Monteith et al., 2012).

It has been reported that chelation of intracellular Ca²⁺ by bis-(O-aminophenoxy)-ethane-N,N,N',N'-tetra-acetoxymethyl ester (BAPTA_{AM}) induces HIF-1 α accumulation in the neuroblastoma cell line SH-SY5Y (Berchner-Pfannschmidt et al., 2004). In our work, an EGTA-induced reduction in the intracellular Ca²⁺ levels and inhibition of TRPC6 suppressed the hypoxic accumulation of HIF-1 α in human glioma cell lines. It is possible that Ca²⁺ from different sources might have different effects on HIF-1 α accumulation. Alternatively, these differences possibly result from different pools of Ca²⁺ that are activated under hypoxia in different cell lines.

In conclusion, we have shown the important role of TRPC6 channels in regulation of hypoxia-induced HIF-1 α accumulation in glioma cells. During hypoxia, release of IGF-1 activates TRPC6 channels through the IGF-1R–PLC γ –IP₃R pathway. The Ca²⁺ influx through TRPC6 regulates metabolite levels and inhibits PHD activities, leading to rapid HIF-1 α protein accumulation. Our work reveals a new mechanism of how the rapid hydroxylation of HIF-1 α is regulated. Moreover, TRPC6 activation also increases GLUT1 expression to regulate glucose metabolism.

MATERIALS AND METHODS

Cell cultures, reagents and antibodies

The U-251 MG (U251, p53^{-/-}), U-87 MG (U87, p53^{+/+}), human embryonic kidney (HEK) 293 cells and HEK293T cells were purchased from the American Type Culture Collection (ATCC). They were cultured in Dulbecco's modified Eagle medium (DMEM), supplemented with 10% fetal bovine serum, 50 units/ml penicillin and 50 units/ml streptomycin. Cells were treated with the following reagents: ethylene glycol tetraacetic acid (EGTA), SKF96365, mibefradil, nimodipine, D(-)-2-amino-5-phosphonopentanoic acid (D-APV), 6-cyano-7-nitroquinoxaline-2,3-dione (CNQX), cobalt chloride (CoCl₂), 1-oleoyl-2-acetyl-sn-glycerol (OAG), thapsigargin, 2-aminoethyl diphenylborinate (2-APB), MG132 and dimethylxalylglycine N-(methoxyoxoacetyl)-glycine methyl ester (DMOG), all purchased from Sigma; U73122 from Calbiochem; suramin from Santa Cruz Biotechnology; pazopanib, canertinib dihydrochloride and BMS-754807 from MedChem Express; and K252a from Merck. The 3-nitrocoumarin and 7-OH-3-nitrocoumarin were gifts from Renata Tisi and Enzo Martegani (Milano-Bicocca University, Milan, Italy) (He et al., 2012). Recombinant human IGF-1 was from PeptoTech. The primary antibodies used for western blotting were against hydroxy-HIF-1 α (Pro564), phosphorylated Akt (Ser473), phosphorylated p44 and p42 MAPK (ERK1/2) (Thr202/Tyr204), p44/42 MAPK (ERK1/2), phosphorylated 4E-BP1 (Ser65) and phosphorylated p70S6 Kinase (Thr389) (Cell Signaling), all Akt isoforms (Akt1, Akt2 and Akt3) (Santa Cruz Biotechnology), HIF-2 α , HIF-1 β , GLUT1, LDHA and LDHB (Novus Biologicals), TRPC6, the HA tag, β -actin, α -tubulin and GAPDH (Sigma), and HIF-1 α (BD Transduction Laboratories). The neutralizing antibody against IGF-1R α was from Santa Cruz Biotechnology.

Plasmids, adenoviral and lentiviral vectors

The full-length sequences of HIF-1 α and its mutants from pcDNA3 or fumarase from pEGFP-N3 were cloned into pCAGGS. An HA tag was fused to the C-terminus of the proteins, which can be used to separate recombinant overexpressed proteins from wild-type proteins.

Adenovirus expressing GFP, dominant-negative TRPC6 (DNC6) or wild-type TRPC6 (WTC6) and lentivirus-based short hairpin RNA (shRNA) constructs were produced as previously described (Ding et al., 2010). In DNC6, three mutations (L678A, F679A, and W680A) were introduced to block ion influx through TRPC6 channels (Hofmann et al., 2002). The shRNA sequences targeting TRPC6 and fumarase are listed in supplementary material Table S1. Target sequences are underlined.

Induction of hypoxia

To induce hypoxia, the cell cultures were placed in a chamber (Forma Scientific) purged by gas mixture (1% O₂, 5% CO₂ and 94% N₂) for different time periods at 37°C.

Western blotting

The methods for samples preparation, electrophoresis and band density quantification were as previously described (Ding et al., 2010). Briefly, total proteins of U251 and U87 cells were extracted using SDS lysis buffer (2% SDS, 10% glycerol, 0.1 mM dithiothreitol and 0.2 M Tris-HCl pH 6.8). In experiments where HIF-1 α protein was measured, proteins were extracted from cells within 10 s by rapidly removing the medium and scraping the cells into SDS lysis buffer. Protein extracts were subjected to SDS-PAGE and transferred to polyvinylidene fluoride membrane (GE Healthcare), and probed with primary antibodies at 4°C overnight and secondary antibodies

at room temperature for 2 h. Bands were visualized by ECL (GE Healthcare). Band densities were determined by the ImageQuant software (GE Healthcare). The relative amount of proteins was determined by normalizing the density of interest to that of the internal loading control, and then normalizing to those in the control group. The ratio of hydroxyl-HIF-1 α (Pro564) to HIF-1 α (Hyp564:HIF-1 α) was used to evaluate the hydroxylation levels of HIF-1 α . Change in hydroxylation levels of HIF-1 α during hypoxia was defined as the Hyp564:HIF-1 α ratio [(Hyp564/HIF-1 α during hypoxia)/(Hyp564/HIF-1 α in normoxia)].

Reverse transcription and quantitative real-time PCR

Total RNA extracted from U251 and U87 cells using TRIzol (Invitrogen) was reverse-transcribed to first-strand cDNA in a 20 μ l reaction volume containing 5 μ g RNA, random primer, dNTP, RNAase inhibitor and M-MuLV reverse transcriptase (Fermentas).

Quantitative real-time PCR (qPCR) was performed with SYBR Premix Ex Taq Kit (Takara) and analyzed on a Rotor-Gene Q (Qiagen). The qPCR conditions were as follows: 95°C, 10 min and 40 cycles of 95°C, 10 s, 60°C, 15 s, 72°C, 20 s. Quantification was performed by using the comparative Ct ($\Delta\Delta$ Ct) method according to manufacturer's instructions. The primers used for qPCR are listed in supplementary material Table S1.

Ca²⁺ imaging

Intracellular Ca²⁺ concentration ([Ca²⁺]_i) was recorded using Fura-2 AM (Invitrogen). A total of 5 \times 10⁴ U87 cells were seeded on each coverslip and loaded with 5 μ M Fura-2 AM for 30 min at 37°C. The normal extracellular solution for Ca²⁺ imaging contained (in mM): NaCl 135, KCl 5.4, CaCl₂ 1.8, MgCl₂ 1.3, HEPES 10, D-Glucose 10, at pH 7.4. The zero Ca²⁺ extracellular solution contained (in mM): NaCl 135, KCl 5.4, EGTA 4, MgCl₂ 1.3, HEPES 10, D-Glucose 10, at pH 7.4. Cells were washed twice with extracellular solution and then put into the recording chamber. Hypoxic solution was achieved by bubbling with the gas mixture 1% O₂, 5% CO₂ and 94% N₂ for at least 20 min before cell perfusion and by blowing the gas over the surface of the recording chamber using a modified airtight lid. Images were acquired using a Nikon Eclipse TE2000-E microscope with dual excitations at 340 and 380 nm and emission was collected at 500 nm every 6 s. [Ca²⁺]_i was calculated on the basis of the Grynkiewicz Eqn formula: [Ca²⁺]_i=K_D×B×(R−R_{min})/(R_{max}−R), where K_D is the dissociation constant for Fura-2 for Ca²⁺ (220 nM), B is the ratio of fluorescence intensity of 380 nm at zero and saturating Ca²⁺ concentrations, R is the ratio of fluorescence intensity at two different wavelengths (340 nm/380 nm), and R_{min} and R_{max} are the ratios at zero and saturating Ca²⁺ concentrations, respectively. The [Ca²⁺]_i peak area represents the Ca²⁺ elevation (Sukumaran et al., 2015).

Enzyme-linked immunosorbent assay

The U87 cells were seeded in 35-mm plates and incubated in the normal extracellular solution for Ca²⁺ imaging prior to ELISA. The supernatants were collected 4 h after hypoxia, and BDNF and IGF-1 levels were quantified by the colorimetric assay (RayBiotech), according to the manufacturer's instructions. Only values within the linear range of the standard curve were used to determine the concentration of BDNF or IGF-1.

NMR analysis of intracellular metabolites

To analyze intracellular levels of metabolites, glioma cells from four 10-cm plates were transfected and extracted. NMR was used to measure the levels of α -ketoglutarate, fumarate and lactate as described previously (Isaacs et al., 2005). Briefly, the cells were rinsed twice with PBS and lysed in 450 μ l of 6% cold perchloric acid plus 50 μ l of 1 mM sodium 3-trimethylsilyl-2, 2, 3, 3-tetradeuteriopropionate (Sigma; served as the internal control). The cell lysates were centrifuged at 15,700 *g* for 10 min at 4°C. The supernatants containing the metabolites were transferred to new tubes, while the remaining protein precipitates were used for quantification. The supernatants were neutralized with 10% potassium hydroxide, and the samples were centrifuged at 15,700 *g* for 10 min at 4°C to remove the salt precipitates. A total of 30 μ l deuterium oxide was added to 570 μ l neutralized cell extracts, which was placed in a 5-mm NMR tube. ¹H NMR spectra were obtained by using a Bruker 400 MHz spectrometer with

repetition time of 6.3 s and 384 averages. Metabolite levels were normalized to the corresponding amount of protein. The metabolites levels in cells infected with GFP were set as 1.0, and this value was used to calculate the relative metabolites levels in cells infected with DNC6.

GC-MS analysis of α -ketoglutarate and succinate

The intracellular levels of α -ketoglutarate and succinate were analyzed by GC-MS as previously described (Zhang et al., 2015). Briefly, glioma cells were rinsed with PBS, detached with trypsin and subjected to centrifugation at 100 *g* for 5 min, and stored at −80°C for subsequent analysis (cells were divided into two groups, one group was for measurement and the other was for cell counting and normalization).

Cell pellets were re-suspended in 400 μ l 50% cold methanol containing internal standard (100 μ M L-norvaline), left to freeze on dry ice for 30 min, and then thawed on ice for 10 min. A total of 300 μ l chloroform was added to each sample, then the samples were vortexed and centrifuged at 15,700 *g* for 10 min at 4°C. The methanol extract layer was collected, dried by centrifugal evaporation and stored at −80°C before analysis.

Dried methanol extracts were derivatized first by addition of 70 μ l 20 mg/ml O-isobutylhydroxylamine hydrochloride and incubation for 20 min at 85°C. After cooling, 30 μ l N-tert-butyltrimethylsilyl-N-methyltrifluoroacetamide (Sigma) was added and samples were re-incubated for 60 min at 85°C before centrifugation at 15,700 *g* for 5 min at 4°C. The supernatants were transferred to autosampler vials for GC-MS (Shimadzu QP 2010 GC tandem quadrupole mass spectrometer) analysis.

Glucose uptake assay

U87 cells infected with adenovirus expressing GFP or DNC6 were transfected with or without pCAGGS-HIF-1 α -HA. After 24 h, the medium was replenished and cells were cultured in normoxic or hypoxic conditions for an additional 24 h. The intracellular glucose levels were measured using the glucose assay kit (BioVision) according to manufacturer's protocol and levels were normalized to cell numbers per sample.

Human data sets

The data of mRNA expression levels of TRPC6, SLC2A1, LDHA and LDHB in human glioblastoma from The Cancer Genome Atlas (TCGA) database were obtained and analyzed by using the cBioPortal for Cancer Genomics (Cerami et al., 2012; Gao et al., 2013).

Statistics

Statistics was carried out using Microsoft Excel and GraphPad Prism to evaluate the differences between different groups. Statistical analysis was performed using Student's *t*-tests or ANOVA (used in cases where there are more than two groups). All results are shown as mean±s.e.m. from three or more independent experiments. *P*-values less than 0.05 were considered statistically significant. One asterisk, two asterisks, three asterisks and four asterisks represent *P*<0.05, *P*<0.01, *P*<0.001 and *P*<0.0001, respectively.

Acknowledgements

We are grateful to C. Pugh for the HIF-1 α construct, L. A. Aaltonen for the FH-pEGFP-N3 construct and K. L. Guan for comments.

Competing interests

The authors declare no competing or financial interests.

Author contributions

S.L. designed and performed most experiments; J.W., Y. Wei., Y.L. and X.D. performed western blots and PCR experiments; S.L. wrote the manuscript; B.D., Y.X. and Y. Wang supervised the study and wrote the manuscript.

Funding

This work was supported by grants from the National Natural Science Foundation of China [grant numbers 81130081, 81371454 and 81172180].

Supplementary material

Supplementary material available online at <http://jcs.biologists.org/lookup/suppl/doi:10.1242/jcs.173161/-/DC1>

References

- Ambalavanan, N., Bulger, A. and Philips, J. B. III (1999). Hypoxia-induced release of peptide growth factors from neonatal porcine pulmonary artery smooth muscle cells. *Biol. Neonate* **76**, 311–319.
- Andersson, K.-E., Gratzke, C. and Hedlund, P. (2010). The role of the transient receptor potential (TRP) superfamily of cation-selective channels in the management of the overactive bladder. *BJU Int.* **106**, 1114–1127.
- Berchner-Pfannschmidt, U., Petrat, F., Doege, K., Trinidad, B., Freitag, P., Metzner, E., de Groot, H. and Fandrey, J. (2004). Chelation of cellular calcium modulates hypoxia-inducible gene expression through activation of hypoxia-inducible factor-1alpha. *J. Biol. Chem.* **279**, 44976–44986.
- Berra, E., Benizri, E., Ginouvès, A., Volmat, V., Roux, D. and Pouyssegur, J. (2003). HIF prolyl-hydroxylase 2 is the key oxygen sensor setting low steady-state levels of HIF-1 alpha in normoxia. *EMBO J.* **22**, 4082–4090.
- Benizri, E., Ginouvès, A. and Berra, E. (2008). The magic of the hypoxia-signaling cascade. *Cell. Mol. Life Sci.* **65**, 1133–1149.
- Bréchar, S., Melchior, C., Plançon, S., Schenten, V. and Tschirhart, E. J. (2008). Store-operated Ca²⁺ channels formed by TRPC1, TRPC6 and Orai1 and non-store-operated channels formed by TRPC3 are involved in the regulation of NADPH oxidase in HL-60 granulocytes. *Cell Calcium* **44**, 492–506.
- Brennan, C. W., Verhaak, R. G. W., McKenna, A., Campos, B., Noushmehr, H., Salama, S. R., Zheng, S., Chakravarty, D., Sanborn, J. Z., Berman, S. H. et al. (2013). The somatic genomic landscape of glioblastoma. *Cell* **155**, 462–477.
- Cai, R., Ding, X., Zhou, K., Shi, Y., Ge, R., Ren, G., Jin, Y. and Wang, Y. (2009). Blockade of TRPC6 channels induced G2/M phase arrest and suppressed growth in human gastric cancer cells. *Int. J. Cancer* **125**, 2281–2287.
- Cai, Q. L., Verma, S. C., Kumar, P., Ma, M. and Robertson, E. S. (2010). Hypoxia inactivates the VHL tumor suppressor through PIASy-mediated SUMO modification. *PLoS ONE* **5**, e9720.
- Cairns, R. A., Harris, I. S. and Mak, T. W. (2011). Regulation of cancer cell metabolism. *Nat. Rev. Cancer* **11**, 85–95.
- Cerami, E., Gao, J., Dogrusoz, U., Gross, B. E., Sumer, S. O., Aksoy, B. A., Jacobsen, A., Byrne, C. J., Heuer, M. L., Larsson, E. et al. (2012). The cBio cancer genomics portal: an open platform for exploring multidimensional cancer genomics data. *Cancer Discov.* **2**, 401–404.
- Chan, D. A., Sutphin, P. D., Denko, N. C. and Giaccia, A. J. (2002). Role of prolyl hydroxylation in oncogenically stabilized hypoxia-inducible factor-1 alpha. *J. Biol. Chem.* **277**, 40112–40117.
- Chan, D. A., Sutphin, P. D., Nguyen, P., Turcotte, S., Lai, E. W., Banh, A., Reynolds, G. E., Chi, J.-T., Wu, J., Solow-Cordero, D. E. et al. (2011). Targeting GLUT1 and the Warburg effect in renal cell carcinoma by chemical synthetic lethality. *Sci. Transl. Med.* **3**, 94ra70.
- Charitou, P., Rodriguez-Colman, M., Gerrits, J., van Triest, M., Groot Koerkamp, M., Hornsveld, M., Holstege, F., Verhoeven-Duif, N. M. and Burgering, B. M. T. (2015). FOXOs support the metabolic requirements of normal and tumor cells by promoting IDH1 expression. *EMBO Rep.* **16**, 456–466.
- Chigurupati, S., Venkataraman, R., Barrera, D., Naganathan, A., Madan, M., Paul, L., Pattisapu, J. V., Kyriazis, G. A., Sugaya, K., Bushnev, S. et al. (2010). Receptor channel TRPC6 is a key mediator of notch-driven glioblastoma growth and invasiveness. *Cancer Res.* **70**, 418–427.
- DeBerardinis, R. J. and Thompson, C. B. (2012). Cellular metabolism and disease: what do metabolic outliers teach us? *Cell* **148**, 1132–1144.
- Ding, X., He, Z., Zhou, K., Cheng, J., Yao, H., Lu, D., Cai, R., Jin, Y., Dong, B., Xu, Y. et al. (2010). Essential role of TRPC6 channels in G2/M phase transition and development of human glioma. *J. Natl. Cancer Inst.* **102**, 1052–1068.
- Dupont, G., Combettes, L., Bird, G. S. and Putney, J. W. (2011). Calcium oscillations. *Cold Spring Harb. Perspect. Biol.* **3**, a004226.
- Faubert, B., Boily, G., Izreig, S., Griss, T., Samborska, B., Dong, Z., Dupuy, F., Chambers, C., Fuerth, B. J., Viollet, B. et al. (2013). AMPK is a negative regulator of the Warburg effect and suppresses tumor growth in vivo. *Cell Metab.* **17**, 113–124.
- Ferrer, C. M., Lynch, T. P., Sodi, V. L., Falcone, J. N., Schwab, L. P., Peacock, D. L., Vocadlo, D. J., Seagroves, T. N. and Reginato, M. J. (2014). O-GlcNAcylation regulates cancer metabolism and survival stress signaling via regulation of the HIF-1 pathway. *Mol. Cell* **54**, 820–831.
- Galban, S. and Gorospe, M. (2009). Factors interacting with HIF-1alpha mRNA: novel therapeutic targets. *Curr. Pharm. Des.* **15**, 3853–3860.
- Gao, J., Aksoy, B. A., Dogrusoz, U., Dresdner, G., Gross, B., Sumer, S. O., Sun, Y. C., Jacobsen, A., Sinha, R., Larsson, E. et al. (2013). Integrative analysis of complex cancer genomics and clinical profiles using the cBioPortal. *Sci. Signal.* **6**, pl1.
- Ghezzi, P., Dinarello, C. A., Bianchi, M., Rosandich, M. E., Repine, J. E. and White, C. W. (1991). Hypoxia increases production of interleukin-1 and tumor necrosis factor by human mononuclear cells. *Cytokine* **3**, 189–194.
- Gunter, T. E., Buntinas, L., Sparagna, G., Eliseev, R. and Gunter, K. (2000). Mitochondrial calcium transport: mechanisms and functions. *Cell Calcium* **28**, 285–296.
- He, Z., Jia, C., Feng, S., Zhou, K., Tai, Y., Bai, X. and Wang, Y. (2012). TRPC5 channel is the mediator of neurotrophin-3 in regulating dendritic growth via CaMKII alpha in rat hippocampal neurons. *J. Neurosci.* **32**, 9383–9395.
- Hofmann, T., Schaefer, M., Schultz, G. and Gudermann, T. (2002). Subunit composition of mammalian transient receptor potential channels in living cells. *Proc. Natl. Acad. Sci. USA* **99**, 7461–7466.
- Hu, Q. and Ziegelstein, R. C. (2000). Hypoxia/reoxygenation stimulates intracellular calcium oscillations in human aortic endothelial cells. *Circulation* **102**, 2541–2547.
- Hui, A. S., Bauer, A. L., Striet, J. B., Schnell, P. O. and Czyzyk-Krzeska, M. F. (2006). Calcium signaling stimulates translation of HIF-alpha during hypoxia. *FASEB J.* **20**, 466–475.
- Hwang, G.-S., Wang, S.-W., Tseng, W.-M., Yu, C.-H. and Wang, P. S. (2007). Effect of hypoxia on the release of vascular endothelial growth factor and testosterone in mouse TM3 Leydig cells. *Am. J. Physiol. Endocrinol. Metab.* **292**, E1763–E1769.
- Isaacs, J. S., Jung, Y. J., Mole, D. R., Lee, S., Torres-Cabala, C., Chung, Y.-L., Merino, M., Trepel, J., Zbar, B., Toro, J. et al. (2005). HIF overexpression correlates with allelic loss of fumarate hydratase in renal cancer: novel role of fumarate in regulation of HIF stability. *Cancer Cell* **8**, 143–153.
- Jia, Y., Zhou, J., Tai, Y. and Wang, Y. (2007). TRPC channels promote cerebellar granule neuron survival. *Nat. Neurosci.* **10**, 559–567.
- Jin, S., Chen, H. G., Zhu, L. P., Liu, S. Y., Wang, D. X. and Hu, Q. H. (2005). Subacute mild hypoxia increases histamine-stimulated calcium oscillation frequency in pulmonary artery endothelial cells. *Prog. Biochem. Biophys.* **32**, 551–556.
- Kaelin, W. G. and McKnight, S. L. (2013). Influence of metabolism on epigenetics and disease. *Cell* **153**, 56–69.
- Kageyama, Y., Koshiji, M., To, K. K., Tian, Y. M., Ratcliffe, P. J. and Huang, L. E. (2004). Leu-574 of human HIF-1alpha is a molecular determinant of prolyl hydroxylation. *FASEB J.* **18**, 1028–1030.
- Koppenol, W. H., Bounds, P. L. and Dang, C. V. (2011). Otto Warburg's contributions to current concepts of cancer metabolism. *Nat. Rev. Cancer* **11**, 325–337.
- Krieg, A. J., Rankin, E. B., Chan, D., Razorenova, O., Fernandez, S. and Giaccia, A. J. (2010). Regulation of the histone demethylase JMJD1A by hypoxia-inducible factor 1 alpha enhances hypoxic gene expression and tumor growth. *Mol. Cell. Biol.* **30**, 344–353.
- Kwon, J., Stephan, S., Mukhopadhyay, A., Muders, M. H., Dutta, S. K., Lau, J. S. and Mukhopadhyay, D. (2009). Insulin receptor substrate-2 mediated insulin-like growth factor-i receptor overexpression in pancreatic adenocarcinoma through protein kinase C delta. *Cancer Res.* **69**, 1350–1357.
- Lemmon, M. A. and Schlessinger, J. (2010). Cell signaling by receptor tyrosine kinases. *Cell* **141**, 1117–1134.
- Li, Y., Jia, Y.-C., Cui, K., Li, N., Zheng, Z.-Y., Wang, Y.-z. and Yuan, X.-b. (2005). Essential role of TRPC channels in the guidance of nerve growth cones by brain-derived neurotrophic factor. *Nature* **434**, 894–898.
- Liao, C., Yang, H., Zhang, R., Sun, H., Zhao, B., Gao, C., Zhu, F. and Jiao, J. (2012). The upregulation of TRPC6 contributes to Ca²⁺ signaling and actin assembly in human mesangial cells after chronic hypoxia. *Biochem. Biophys. Res. Commun.* **421**, 750–756.
- Lin, M. J., Leung, G. P. H., Zhang, W. M., Yang, X. R., Yip, K. P., Tse, C. M. and Sham, J. S. K. (2004). Chronic hypoxia-induced upregulation of store-operated and receptor-operated Ca²⁺ channels in pulmonary arterial smooth muscle cells - A novel mechanism of hypoxic pulmonary hypertension. *Circ. Res.* **95**, 496–505.
- Liu, W., Xin, H., Eckert, D. T., Brown, J. A. and Gnarr, J. R. (2011). Hypoxia and cell cycle regulation of the von Hippel-Lindau tumor suppressor. *Oncogene* **30**, 21–31.
- Marhi, M., Haberichter, T., Brumen, M. and Heinrich, R. (2000). Complex calcium oscillations and the role of mitochondria and cytosolic proteins. *Biosystems* **57**, 75–86.
- Mariani, C. J., Vasanthakumar, A., Madzo, J., Yesilkamal, A., Bhagat, T., Yu, Y., Bhattacharya, S., Wenger, R. H., Cohn, S. L., Nanduri, J. et al. (2014). TET1-Mediated Hydroxymethylation Facilitates Hypoxic Gene Induction in Neuroblastoma. *Cell Rep.* **7**, 1343–1352.
- Meng, F., To, W. K. L. and Gu, Y. (2008). Role of TRP channels and NCX in mediating hypoxia-induced [Ca²⁺]_i elevation in PC12 cells. *Respir. Physiol. Neurobiol.* **164**, 386–393.
- Michiels, C., Arnould, T. and Remacle, J. (2000). Endothelial cell responses to hypoxia: initiation of a cascade of cellular interactions. *Biochim. Biophys. Acta* **1497**, 1–10.
- Monteith, G. R., Davis, F. M. and Roberts-Thomson, S. J. (2012). Calcium channels and pumps in cancer: changes and consequences. *J. Biol. Chem.* **287**, 31666–31673.
- Montell, C. (2005). The TRP superfamily of cation channels. *Sci. Signal.* **2005**, re3.
- Mottet, D., Michel, G., Renard, P., Ninane, N., Raes, M. and Michiels, C. (2003). Role of ERK and calcium in the hypoxia-induced activation of HIF-1. *J. Cell Physiol.* **194**, 30–44.
- Mouta Carreira, C., Landriscina, M., Bellum, S., Prudovsky, I. and Maciag, T. (2001). The comparative release of FGF1 by hypoxia and temperature stress. *Growth Factors* **18**, 277–285.

- Nichols, B. J. and Denton, R. M.** (1995). Towards the molecular basis for the regulation of mitochondrial dehydrogenases by calcium ions. *Mol. Cell. Biochem.* **149-150**, 203-212.
- Nilius, B. and Voets, T.** (2005). TRP channels: a TR(1)P through a world of multifunctional cation channels. *Pflugers Arch.* **451**, 1-10.
- Nilius, B., Owsianik, G., Voets, T. and Peters, J. A.** (2007). Transient receptor potential cation channels in disease. *Physiol. Rev.* **87**, 165-217.
- Oda, S., Oda, T., Takabuchi, S., Nishi, K., Wakamatsu, T., Tanaka, T., Adachi, T., Fukuda, K., Nohara, R. and Hirota, K.** (2009). The calcium channel blocker cilnidipine selectively suppresses hypoxia-inducible factor 1 activity in vascular cells. *Eur. J. Pharmacol.* **606**, 130-136.
- Oermann, E. K., Wu, J., Guan, K.-L. and Xiong, Y.** (2012). Alterations of metabolic genes and metabolites in cancer. *Semin. Cell Dev. Biol.* **23**, 370-380.
- Ogura, K., Sakata, M., Yamaguchi, M., Kurachi, H. and Murata, Y.** (1999). High concentration of glucose decreases glucose transporter-1 expression in mouse placenta in vitro and in vivo. *J. Endocrinol.* **160**, 443-452.
- Pedersen, S. F., Owsianik, G. and Nilius, B.** (2005). TRP channels: an overview. *Cell Calcium* **38**, 233-252.
- Pollard, P. J. and Ratcliffe, P. J.** (2009). Cancer: puzzling patterns of predisposition. *Science* **324**, 192-194.
- Porras, O. H., Ruminot, I., Loaiza, A. and Barros, L. F.** (2008). Na⁺-Ca²⁺ cosignaling in the stimulation of the glucose transporter GLUT1 in cultured Astrocytes. *Glia* **56**, 59-68.
- Quintanilla, R. A., Porras, O. H., Castro, J. and Barros, L. F.** (2000). Cytosolic [Ca²⁺] modulates basal GLUT1 activity and plays a permissive role in its activation by metabolic stress and insulin in rat epithelial cells. *Cell Calcium* **28**, 97-106.
- Satrústegui, J., Pardo, B. and del Arco, A.** (2007). Mitochondrial transporters as novel targets for intracellular calcium signaling. *Physiol. Rev.* **87**, 29-67.
- Sebastián, C., Zwaans, B. M. M., Silberman, D. M., Gymrek, M., Goren, A., Zhong, L., Ram, O., Truelove, J., Guimaraes, A. R., Toiber, D. et al.** (2012). The histone deacetylase SIRT6 is a tumor suppressor that controls cancer metabolism. *Cell* **151**, 1185-1199.
- Semenza, G. L.** (2007). Hypoxia-inducible factor 1 (HIF-1) pathway. *Sci. STKE* **2007**, cm8.
- Sharp, F. R. and Bernardin, M.** (2004). HIF1 and oxygen sensing in the brain. *Nat. Rev. Neurosci.* **5**, 437-448.
- Shi, Y., Ding, X., He, Z.-H., Zhou, K.-C., Wang, Q. and Wang, Y.-Z.** (2009). Critical role of TRPC6 channels in G2 phase transition and the development of human oesophageal cancer. *Gut* **58**, 1443-1450.
- Sneyd, J., Keizer, J. and Sanderson, M. J.** (1995). Mechanisms of calcium oscillations and waves - a quantitative-analysis. *FASEB J.* **9**, 1463-1472.
- Sukumaran, P., Sun, Y., Vyas, M. and Singh, B. B.** (2015). TRPC1-mediated Ca²⁺ entry is essential for the regulation of hypoxia and nutrient depletion-dependent autophagy. *Cell Death Dis.* **6**, e1674.
- Tai, Y., Feng, S., Ge, R., Du, W., Zhang, X., He, Z. and Wang, Y.** (2008). TRPC6 channels promote dendritic growth via the CaMKIV-CREB pathway. *J. Cell Sci.* **121**, 2301-2307.
- Toescu, E. C.** (2004). Hypoxia sensing and pathways of cytosolic Ca²⁺ increases. *Cell Calcium* **36**, 187-199.
- Vander Heiden, M. G., Cantley, L. C. and Thompson, C. B.** (2009). Understanding the Warburg effect: the metabolic requirements of cell proliferation. *Science* **324**, 1029-1033.
- Wang, J., Weigand, L., Lu, W., Sylvester, J. T., Semenza, G. L. and Shimoda, L. A.** (2006). Hypoxia inducible factor 1 mediates hypoxia-induced TRPC expression and elevated intracellular Ca²⁺ in pulmonary arterial smooth muscle cells. *Circ. Res.* **98**, 1528-1537.
- Warnken, M., Reitzenstein, U., Sommer, A., Fuhrmann, M., Mayer, P., Enzmann, H., Juergens, U. R. and Racké, K.** (2010). Characterization of proliferative effects of insulin, insulin analogues and insulin-like growth factor-1 (IGF-1) in human lung fibroblasts. *Naunyn Schmiedebergs Arch. Pharmacol.* **382**, 511-524.
- Wertheimer, E., Sasson, S., Cerasi, E. and Ben-Neriah, Y.** (1991). The ubiquitous glucose transporter glut-1 belongs to the glucose-regulated protein family of stress-inducible proteins. *Proc. Natl. Acad. Sci. USA* **88**, 2525-2529.
- Xu, W., Yang, H., Liu, Y., Yang, Y., Wang, P., Kim, S.-H., Ito, S., Yang, C., Xiao, M.-T., Liu, L.-x. et al.** (2011). Oncometabolite 2-hydroxyglutarate is a competitive inhibitor of alpha-ketoglutarate-dependent dioxygenases. *Cancer Cell* **19**, 17-30.
- Yang, F., Zhang, H., Mei, Y. and Wu, M.** (2014). Reciprocal regulation of HIF-1alpha and lincRNA-p21 modulates the Warburg effect. *Mol. Cell* **53**, 88-100.
- Zhang, G., Yang, P., Guo, P., Miele, L., Sarkar, F. H., Wang, Z. and Zhou, Q.** (2013). Unraveling the mystery of cancer metabolism in the genesis of tumor-initiating cells and development of cancer. *Biochim. Biophys. Acta* **1836**, 49-59.
- Zhang, D., Wang, Y., Shi, Z., Liu, J., Sun, P., Hou, X., Zhang, J., Zhao, S., Zhou, B. P. and Mi, J.** (2015). Metabolic reprogramming of cancer-associated fibroblasts by IDH3 alpha downregulation. *Cell Rep.* **10**, 1335-1348.
- Zhao, S., Lin, Y., Xu, W., Jiang, W., Zha, Z., Wang, P., Yu, W., Li, Z., Gong, L., Peng, Y. et al.** (2009). Glioma-derived mutations in IDH1 dominantly inhibit IDH1 catalytic activity and induce HIF-1alpha. *Science* **324**, 261-265.



Special Issue on 3D Cell Biology

Call for papers

Submission deadline: January 16th, 2016

Journal of Cell Science